DOI 10.1007/s11204-018-9513-5
Soil Mechanics and Foundation Engineering, Vol. 55, No. 2, May, 2018 (Russian Original No. 2, March-April, 2018)

EXPERIMENTAL INVESTIGATIONS

BEHAVIORS OF EMBANKMENT ON PVD-IMPROVED HAIPHONG CLAY

UDC 624.138:624.152.612

Jang W.Y.
GS Engineering & Construction Co., Ltd., Seoul, South Korea.

This paper presents the behaviors of embankments on clay deposits improved by prefabricated vertical drains (PVD) in the north-east coastal plain of Vietnam. The deposit consists of soft Holocene clay (approximately 20 m) and stiff Pleistocene clay (approximately 20 m) on a thick sand layer. PVDs with various spacing were fully installed into the soft clay. Settlement behaviors mostly show a reverse-S curve that consists of three phases: small recompression, rapid and large settlement, and delayed settlement. When the spacing is smaller than 1.0 m, the recompression behavior disappears because of soil disturbance during installation. A nearly elastic behavior is observed during construction; thus, the ratios of lateral displacement to settlement (0.02-0.13) and of the excess pore pressure to the applied pressure (0.1-0.7) are significantly small.

Introduction

The Hanoi Haiphong (Vietnam) express highway (44 m wide and 105.5 km long) connects two big cities in the northern part of the country. The highway passes through a wide coastal plain where thick clay layers overlying a sand layer are formed. Most parts of the route were partially improved using prefabricated vertical drains (PVD), in which various spacing, installed depths, fill heights, and loading rates were adopted. However, soil improvement was designed based on poor ground investigation, in which the local technology for sampling and soil testing was not well developed. Few well-documented reports and research papers related to soil improvement in the area are available. The circumstances of the country are different from those of neighboring countries in the same tropical area [1-6] Therefore, reliable investigation of the geotechnical characteristics of the clay deposits and comprehensive observation of the in situ soil behaviors that occurred during ground improvement in the area are necessary.

This paper presents the field monitoring results at several locations in the highway route, as well as the basic geotechnical properties of the soil deposit, field instruments, and details of the ground improvement. Behaviors of embankments were inclusively evaluated using the monitored settlement, lateral displacement, and excess pore pressures at every construction stage.

According to the ground investigation that was conducted up to a depth of 60 m, Late Quaternary deposit was formed from top to bottom: soft Holocene clay, stiff Pleistocene clay, and sand (fluvial) layer [7]. The formation was closely related to changes in the seawater levels and river floods [8]. The thickness of the soft clay layer increases from approximately 10 m to 20 m as the location becomes closer to Haiphong City, whereas the stiff clay exhibits an opposite trend (from 40 m to 20 m). In this

Translated from Osnovaniya, Fundamenty i Mekhanika Gruntov, No. 1, p. 35, January-February, 2018.

0038-0741/18/5501-0120

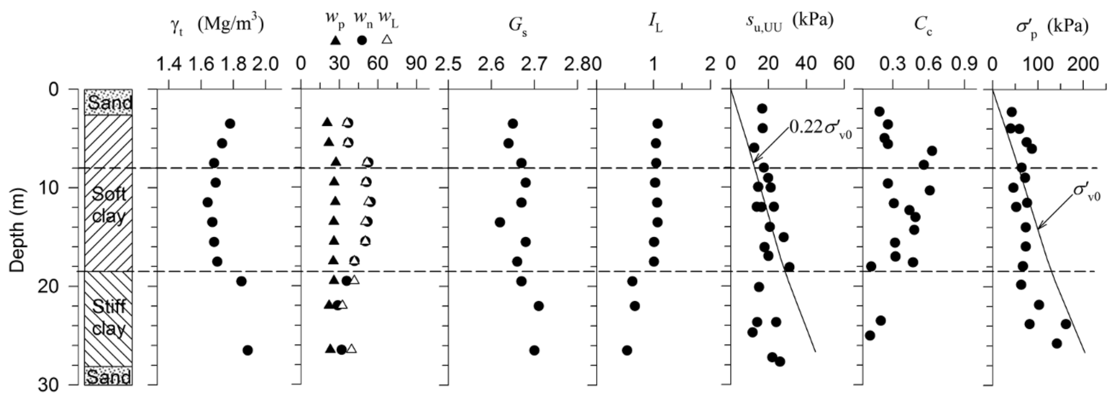

Fig. 1. Basic geotechnical properties.

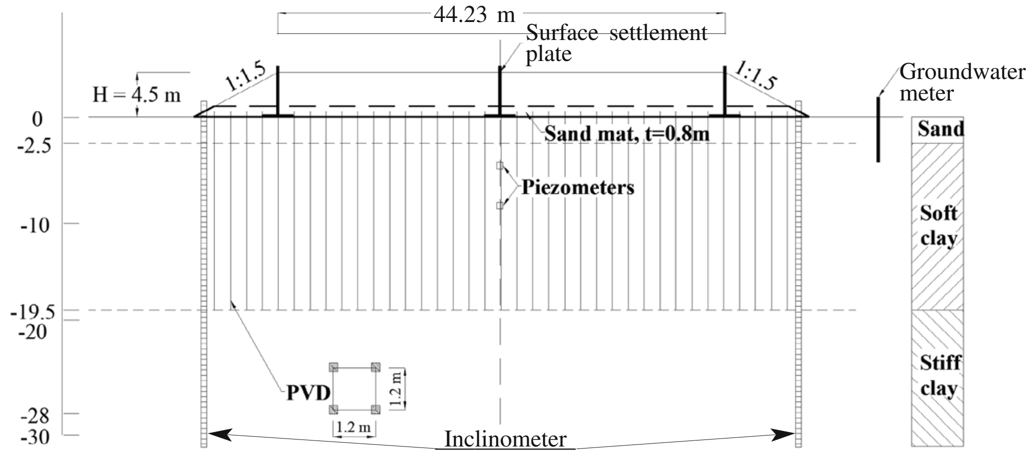

Fig. 2. Typical layout of PVDs and field instrumentation with embankment (Sta. 76+400).

study, a section from Sta. 72+000 to Sta. 81+300 was considered, where the soft clay is relatively thicker than those in most of the remaining locations (20-30 m).

The basic geotechnical property profiles in the section are shown in Fig. 1. The total unit weight γ_t of the soft clay decreased from 1.8 Mg/m^3 at a depth of 2 m to 1.6 Mg/m^3 at a depth of 12 m and thereafter increased up to 1.7 Mg/m^3 at the bottom, whereas those of the stiff clay vary from 1.85 Mg/m^3 to 1.90 Mg/m^3. The water content w_n exhibits a variation opposite to the γ_t. The liquid limit w_L is almost identical to the w_n, whereas the plastic limit w_p, which ranges from 20% to 30%, is relatively constant along the depths. Thus, the liquidity index I_L is almost equal to 1.0 in the soft clay and 0.5 in the stiff clay. The specific gravity G_s of the soft and stiff clays are approximately 2.65 and 2.70, respectively. According to the USCS classification system, the upper (0-8 m), lower soft clay (8-18 m), and the stiff clay are classified as CL, CL-CH, and ML-CL, respectively. The undrained shear strength obtained from the unconsolidated undrained (UU) triaxial compression test $s_{u,UU}$ tends to decrease with depth in the top 8 m; thereafter, the values were close to $0.22\sigma'_{v0}$ [9-11], where σ'_{v0} is the effective overburden stress. The compression index C_c is 0.2-0.3 and 0.3-0.6 for the upper and lower parts of the soft clay, respectively. The apparent preconsolidation stress σ'_p, which was obtained from the standard consolidation test, was higher and lower than the σ'_{v0} for the two layers, respectively. Given that an open tube sampling was used, the samples might be considerably disturbed, thereby resulting in an underestimation of mechanical and compressibility properties.

Figure 2 shows a typical embankment section with PVD and instruments. First, a 0.8 m high horizontal drainage (sand) was placed. Then, a 3 × 100 mm PVD with square spacing that ranges from 0.8 m to 1.6 m was installed up to the bottom of the soft clay layer. The top level of the embankment,

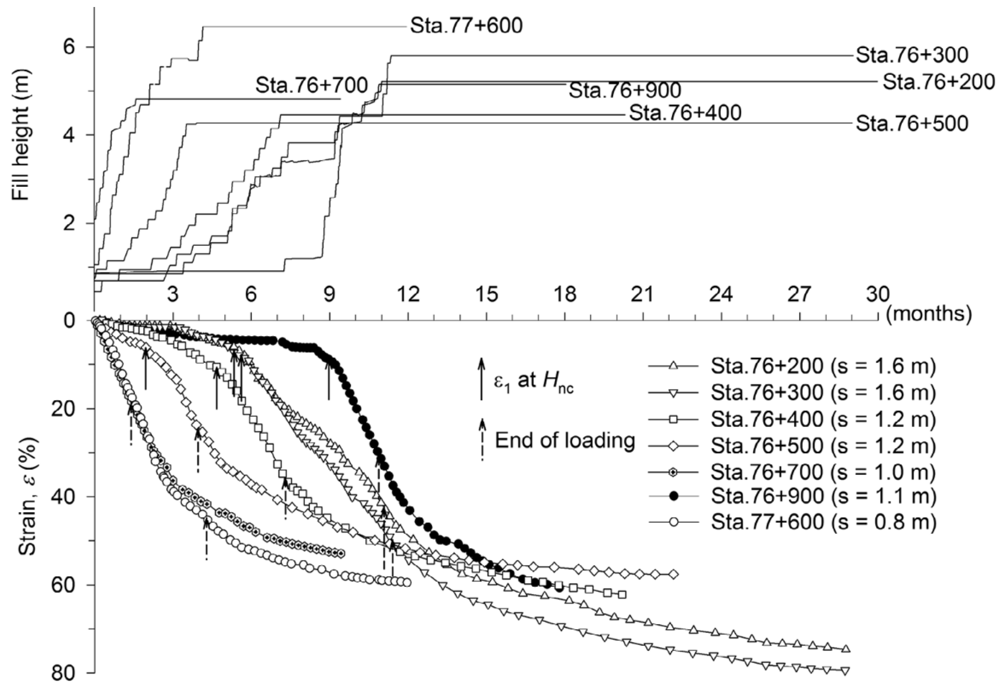

Fig. 3. Time strain plots.

TABLE 1

Station No.	Thickness of soft clay (m)	Fill height (m)	Spacing (m)	PVD length (m)	Loading rate (m/month)	ε_1 at H_{nc} (%)	ε_1 (%)	Total strain (%)
76+200	21.0	5.2	1.6	21.0	0.60	6.6	33.5	74.7
76+300	21.0	5.8	1.6	21.0	0.98	6.9	40.2	79.4
76+400	19.5	4.5	1.2	19.5	0.91	10.4	25.3	62.2
76+500	19.5	4.3	1.2	19.5	1.20	6.2	18.3	57.6
76+700	19.5	4.8	1.0	19.5	1.75	-	21.4	52.9
76+900	21.0	5.2	1.1	21.0	1.38	8.8	22.6	61.4
77+600	23.0	6.4	0.8	23.0	1.77		44.0	59.5

which included the surcharge, was planned to be El. + 4.5 m. The filling materials for the embankment were not supplied on time; thus, the rate of fill placement was different from one location to another. The fill material was mostly sand that was dredged from adjacent rivers. The fill material was then compacted until the relative compaction of 95% was reached, at which the bulk density was approximately 1.95 Mg/m^3. The placement of the horizontal drainage and the determination of embankment height change took a longer period compared with the planned construction schedule.

Field monitoring was conducted using a surface settlement gauge (plate type), piezometer (vibrating-wire type), and inclinometer (multi-stepped type). The instruments were installed after the completion of the PVD installation. Surface settlement gauges were installed at the center and both shoulders of the embankment, with 100 m intervals throughout the route. Piezometers were installed at depths of 5 and 10 m along the centerline, and inclinometers were installed to a depth of 5 m below the stiff clay layer at both toes of the embankment. However, the piezometers and inclinometers were installed only at several locations in the section between Sta. 72+000 and Sta. 81+300.

Field monitoring results

Timelines and settlement behaviors (i.e., strain) at seven locations in the section are shown in Fig. 3. Ground improvement conditions were different at each location (Table 1). Vertical strain behaviors varied depending on the fill height, loading rate, spacing, and thickness of the soft clay layer (rather

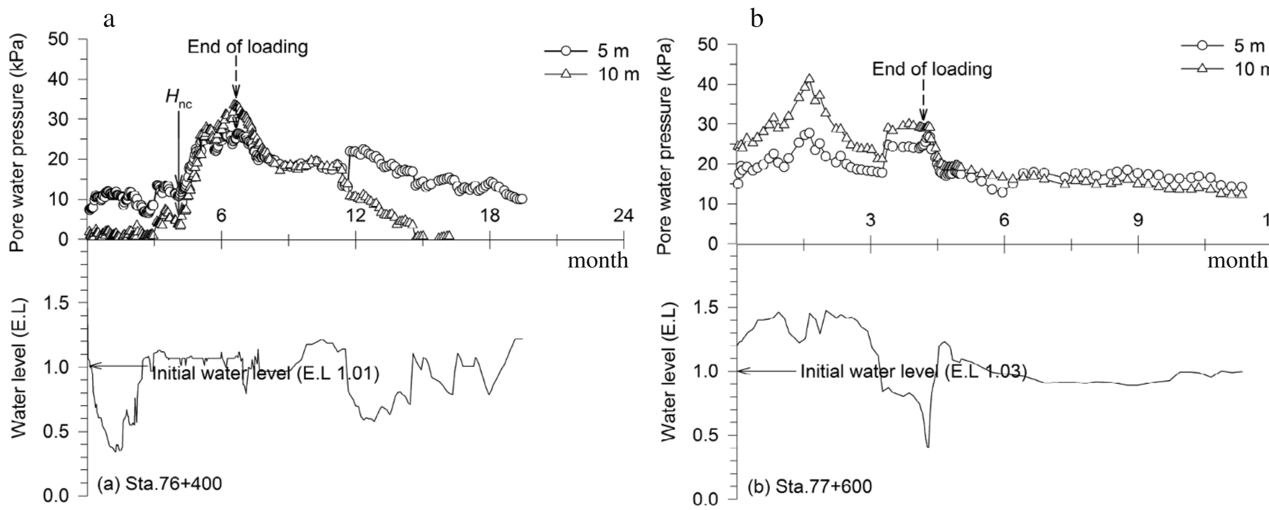

Fig. 4. Measured pore pressure and water level: a) Sta 76+400; b) Sta 77+600.

than those of the stiff clay layer). The settlement behaviors prior to the end of loading showed variations, and post-behaviors exhibited a relatively similar trend.

Most of the time strain curves show a reverse-S shape and can be divided into three phases: a gradual increase during the early stage (phase 1), sudden increase until the loading is ended (phase 2), and moderate and gradual increase after the end of loading (phase 3). However, such behaviors were not exhibited at two locations (Sta. 76+700 and 77+600), where the spacing of PVDs was short and the loading rates were rapid. The fill height during phase 1 is denoted as the threshold height H_{nc}. The underlying soil before and after the H_{nc} behaves as the overconsolidated (OC) and normally consolidated (NC) conditions, respectively [12-13]. Interestingly, strain behaviors during phases 1 and 2 were observed to be almost linear at the first five locations. In Table 1, the strains at each phase are denoted as ε_1, ε_2, and ε_3. The measured strains at several stations are also cited.

Two locations with different time strain behaviors (Sta. 76+400 and Sta.77+600) are considered hereafter. Figure 4 shows the variations in the excess pore pressures u_e and the water levels at the locations. The groundwater level decreased slightly during the dry season in October to December (i.e., t = 0-2 month and 12-14 month) and thereafter rose to a high level. The initial values of u_e at t = 0 varied because the lateral (horizontal) drainage layer was placed at a different time. At two depths at Sta. 76+400, the u_e values did not increase during phase 1, but started to escalate rapidly during phase 2. The ue values during phase 3 reached within 3 months after phase 2 and thereafter decreased at a slow rate. The peak value at the depth of 5 m (27 kPa) is lower than that at the depth of 10 m (33 kPa). By contrast, the u_e values at the two depths of Sta. 77+600 (without phase 1) were different from those of Sta. 76+400. The u_e values at two depths increased to the peak, decreased during phase 2, and decreased gently thereafter during phase 3. The peak value at the depth of 5 m (28 kPa) was also lower than that at the depth of 10 m (41 kPa). Overall, the variations in u_e appeared to be similar to those of the settlements.

The measured lateral displacements at two locations are shown in Fig. 5. Displacements at both locations were similar in shape but different in magnitude. The maximum displacements were observed at a depth of 6 m. As shown in Fig. 5a, the lateral displacement y at Sta. 76+400 is very small (maximum value of 6 mm at a depth of 6 m) during phase 1 (H_{nc} = 2.4 m). Afterward, the displacement continued to increase rapidly to the maximum value of 40 mm during phase 2 (H = 4.5 m) and to the maximum value of 63 mm within the period of one year. By contrast, a large displacement (maximum value of 29 mm at a depth of 6 m) at Sta. 77+600 was observed during the fill placement of 2.3 m. Thereafter, the higher fill placement (H = 6.4 m) accelerated the displacement to the maximum of 86 mm at the end of loading and the maximum of 115 mm within the period of one year.

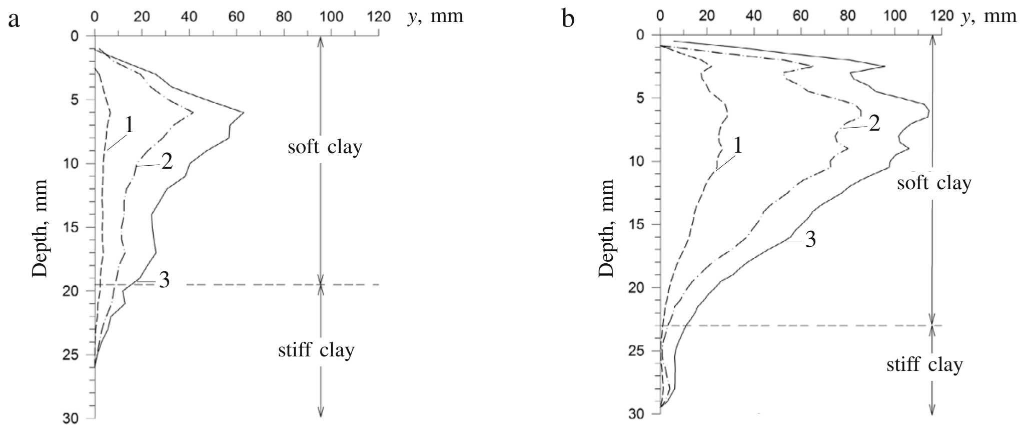

Fig. 5. Measured lateral displacements: a) Sta 76+400; b) Sta 77+600; 1) H_{nc} = 2.4 m; 2) end of loading; 3) 1 year.

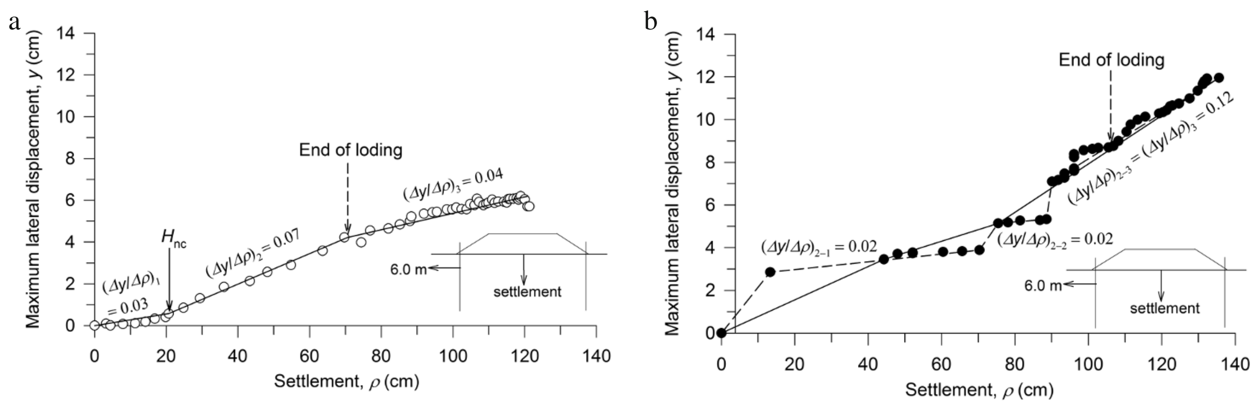

Fig. 6. Relationships between settlement ρ and maximum lateral displacement y: a) Sta 76+400; b) Sta 77+600.

Discussion

The relationships between the maximum lateral displacement (y) and the settlement (ρ) for the two typical cases are shown in Fig. 6. The lateral displacements are very small relative to the settlements. At Sta. 76+400, the slopes ($\Delta y/\Delta\rho$) remarkably changed at the three phases: 0.03, 0.07, and 0.04. The results were qualitatively similar to but quantitatively smaller than those obtained from Canadian clays [14]: $(\Delta y/\Delta\rho)_1 = 0.18 \pm 0.09$, $(\Delta y/\Delta\rho)_2 = 0.91 \pm 0.2$, and $(\Delta y/\Delta\rho)_3 = 0.07 \pm 0.03$ for phases 1, 2, and 3, respectively. The lateral displacements at Sta. 77+600 were larger than those of Sta. 76+400; however, the $\Delta y/\Delta\rho$ ratios were still small. As three steps of loading rates were applied (Fig. 4), the $\Delta y - \Delta\rho$ relationships in phase 2 resulted in three discrete slopes of 0.02 to 0.12. The $(\Delta y/\Delta\rho)_3$ was nearly identical to the third slope of phase 2, $(\Delta y/\Delta\rho)_{2\text{-}3}$. Table 2 shows the y and ρ at several locations. The $\Delta y/\Delta\rho$ values were 0.02-0.13 and 0.04-0.18 for phases 2 and 3, respectively.

At each phase, the relationships of the excess pore pressure (Δu) versus the applied load ($\Delta\sigma$) were evaluated for two typical cases. Figure 7(a) shows the variations in $\Delta u/\Delta\sigma = \overline{B}$ at Sta. 76+400: $\overline{B}_1$ = (–) 4.0 to 0.1 for the phase 1 and $\overline{B}_2 = 0.7$ for phase 2. A similar result was observed at Sta. 76+900.
The ratios during phases 1 and 2 at the locations were significantly smaller than those obtained from the Saint-Alban test fills [12-13]: $\overline{B}_1 = 0.6 - 2.4(z/D - 0.5)^2$ and $\overline{B}_2 = 1.05 \pm 0.15$, where z and D are the depth and the thickness of the clay layer, respectively. In this case, the settlements during the three phases were defined as elastic settlement or recompression, undrained distortion, and consolidation settlement. Similar to those at Sta. 76+400, $\overline{B}_2$ at Sta. 77+600 was mostly between 0.1 and 0.6, where phase 1 disappears (Fig. 7b). Excess pore pressures decreased at both locations after the construction (see Fig. 4).

TABLE 2

Station No.	Method	Spacing (m)	Thickness of soft clay (m)	Fill height (m)	Settlement ρ (cm)	Max. lateral displacement y (cm)	$\Delta y/\Delta\rho$		
							Phase 1	Phase 2	Phase 3
73+900	PVD	0.9	21.5	4.0	63.1	6.9	–	0.13	0.06
76+400	PVD	1.2	19.5	4.5	121.3	5.8	0.03	0.07	0.04
77+600	PVD	0.8	23.0	6.4	135.6	12.0	–	0.08	0.12
79+800	PVD	1.0	35.0	6.6	147.8	9.0	–	0.04	0.18
80+000	Sand drain	1.5	30.0	7.2	187.9	15.2	–	0.06	0.15
80+800	PVD	0.9	35.0	6.2	166.5	16.7	–	0.05	0.08

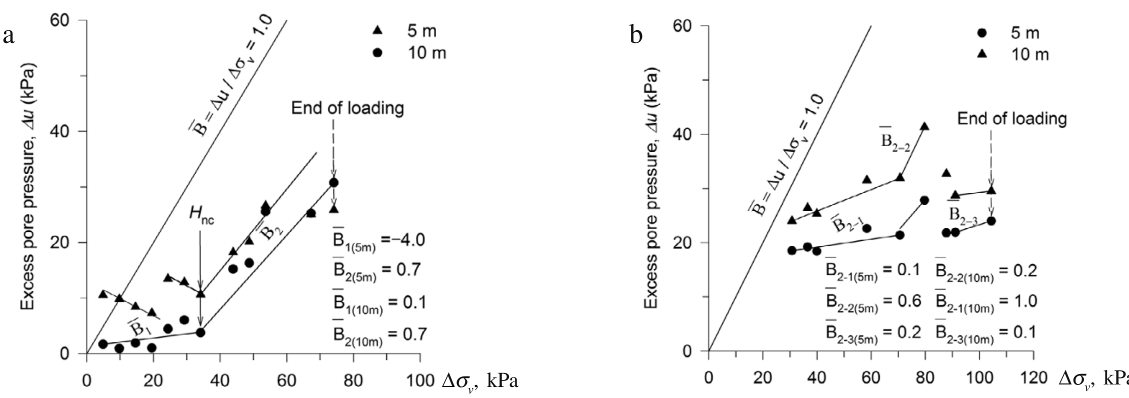

Fig. 7. Pore pressure versus load: a) Sta 76+400; b) Sta 77+600.

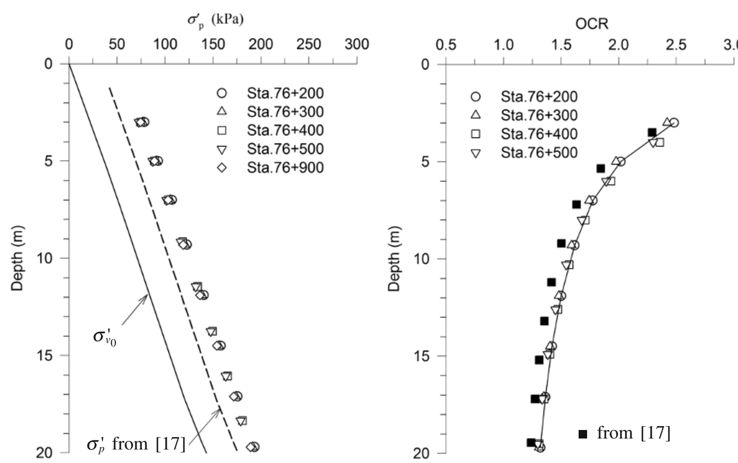

Fig. 8. Apparent preconsolidation pressures and OCR.

The preconsolidation stress obtained from the conventional consolidation test was lower than the effective overburden stress at the depths below 6 m (Fig. 1). As described previously, the underestimation may be caused by sample disturbance and testing method [15]. The apparent preconsolidation stress σ_p' can be estimated using field measurement results [16]. On the basis of the assumption that the embankment is sufficiently wide and the consolidation settlement occurs in the soft clay, and the soil under the centerline may be subjected to almost the same stress increment as the applied (embankment) load, the stress increment $\Delta\sigma$ at the H_{nc} (Fig. 7a) is identical to the value of $(\sigma_p' - \sigma_{v0}')$.

Figure 8 shows that the estimated values of σ_p' and OCR at each depth were slightly higher than those from an empirical equation for the clay [17]: $\sigma_p' = \sigma_{v0}' + 33$ (kPa). The apparent preconsolidation stress σ_p' of clay falls as the loading rates decrease [18]. Thus, the OCR values evaluated using the σ_p' values at each depth is approximately 1.3 2.5, which is slightly lower and higher than the designed values for the upper (2.8) and lower soft clay layers (1.0), respectively. The evaluated OCR distribution with depth is in good agreement with the results of Suzuki and Takeuchi [17].

Conclusions

A 9.3-km-long section with relatively thick soft clay in the Hanoi Haiphong highway constructed across the northeast plain of Vietnam was selected for this study. Embankments with various heights (4.3-6.4 m) were applied at different loading rates (9.2-58.5 kPa/month), and PVDs with different spacing (0.8 1.6 m) were partially installed to improve only the soft clay (~20 m thick). The following significant results were obtained from field monitoring in the section:

Two settlement behavior patterns were observed: a reverse S-shaped curve (i.e., recompression (ρ_1), rapid linear compression (ρ_2), and delayed settlement (ρ_3) behavior) at most stations; and a concave curve (i.e., only with the ρ_2 and ρ_3) at two stations. Recompression occurred until the strain reached 2-4%, at which the critical height of embankments (H_{nc} = 2.2-2.4 m) was evaluated. The lateral displacements beneath the toes of the embankments were significantly small, whereas the values in the concave pattern are significantly larger than those in the reverse-S pattern: mostly, $\Delta y/\Delta\rho \leq 0.1$. The ratios ($\bar{B}$) of the excess pore pressure to the applied pressure were also small: $\bar{B}_1 \leq 0.1$ and $\bar{B}_2$ = 0.1 0.7.

The recompression disappeared at the two stations where the PVD spacing was less than 1.0 m and the loading rate was rapid. This means that the recompression is sensitive to soil disturbance during the installation of mandrels and loading rate. The monitoring-based overconsolidation ratios were evaluated to be within 1.3-2.5, which were considerably greater than those obtained from the consolidation test. The evaluation method of the overconsolidation ratio using H_{nc} is valid and recommendable.

REFERENCE

1. A. Arulrajah, M. W. Bo, J. Chu, and H. Nikraz, "Instrumentation at the Changi land reclamation project, Singapore," *Geotech. Eng.*, **162**, 33-40 (2009).
2. D. T. Bergado, M. C. Alfaro, and A. S. Balasubramaniam, "Improvement of soft Bangkok clay using vertical drains," *Geotext. Geomembr.*, **12**, 615-663 (1993).
3. M. W. Bo, J. Chu, B. K. Low, and V. Choa, "Soil Improvement: Prefabricated Vertical Drain Technique," *ISBN 981-243-044-X*, Thomson Learning, Singapore (2003).
4. J. B. Cox, "Shear strength characteristics of the recent marine clays in South East Asia," J. *S.E. Asian Soc. Soil Eng.*, **1**, 1-28 (1970).
5. J. Chu, M. W. Bo, M. F. Chang, and V. Choa, "Consolidation and permeability properties of Singapore marine clay," *J. Geotech. Geoenviron. Eng.*, **128**, 724-732 (2002).
6. Z. M. Moh, J. D. Neldson, and E. W. Brand, "Strength and deformation behavior of Bangkok clay," *Proc. 7th Int. Conf. Soil Mech. Found. Eng.*, Mexico City, **1**, 287-295 (1969).
7. S. Jusseret, C. Baeteman, and A. Dassargues, "The stratigraphical architecture of the Quaternary deposits as support for hydrogeological modeling of the central zone of Hanoi (Vietnam)," *Geol. Belg.*, **13**, 77-90 (2010).
8. K. Hori, S. Tanabe, Y. Saito, S. Haruyama, V. Nguyen, and A. Kitamura, "Delta initiation and the Holocene sea-level change: Example from the Song Hong (Red River) delta, Vietnam," *Sediment. Geol.*, 164, 237-249 (2004).
9. S.G. Chung, S.K. Kim, Y.J Kang, J.C. Im, and K.N. Prasad, "Failure of a breakwater founded on a thick normally consolidated clay," *Geotechnique*, **56**, 393-409 (2006).
10. G. Mesri, "Discussion on 'New design procedure for stability of soft clays'," *J. GED*, ASCE, **101**, 409-412 (1975).
11. G. Mesri, "A re-evaluation of su(mob) using laboratory shear tests," *Can. Geotech. J.*, **26**, 162-164 (1989).
12. S. Leroueil, F. Tavenas, C. Mieussens, and M. Peignaud, "Construction pore pressures in clay foundations under embankments, Part 2: generalized behavior," *Can. Geotech. J.*, **15**, 66-82 (1978).
13. S. Leroueil, F. Tavenas, B, Trak, P. La Rochelle, and M. Roy, "Construction pore pressures in clay foundations under embankments, Part I: the Saint-Alban test fills," *Can. Geotech. J.*, **15**, 54-65 (1978).
14. F. Tavenas, C. Mieussens, and F. Bourges, "Lateral displacement in clay foundations under embankments," *Can. Geotech. J.*, **16**, 532-550 (1979).
15. S.G. Chung, H.J. Kweon, and W.Y Jang, "Observational method for field performance of prefabricated vertical drains," *Geotext. Geomembr.*, **42**, 405-416 (2014).
16. P. Morin, S. Leroueil, and L. Samson, "Preconsolidation pressure of Champlain clays. Part I. In-situ determination, *Can. Geotech. J.*, **20**, 782-802 (1983).
17. K. Suzuki and H. Takeuchi, "Performance of band shaped vertical drain for soft Hai Phong clay," *Soils Found.*, **48**, 577-585 (2008).
18. S. Leroueil, F. Tavenas, L. Samson, and P. Morin, "Preconsolidation pressure of Champlain clays Part II. Laboratory determination," *Can. Geotech. J.*, **20**, 803-816 (1983).